Modeling *Pseudomonas aeruginosa* Aggregates:

A Multi-Scale Simulation Approach to Understanding Growth Dynamics

A Dissertation
Presented to
The Academic Faculty

by

Karthik Krishnan
Georgia Institute of Technology
kkrishnan38@gatech.edu

In Partial Fulfillment of the Requirements for the Degree
of Computer Science in the College of Computing

Approved by

Dr. Samuel Brown
School of Biological Sciences
Georgia Institute of Technology

Dr. Nisha Chandramoorthy
Department of Statistics
University of Chicago

Acknowledgements

This work was made possible by my project lead and supervisor, Dr. Sarah Sundius, and my P.I.'s, Dr. Sam Brown and Dr. Rachel Kuske. I am very grateful for their mentorship, feedback and patience. They have inspired me to approach complex scientific challenges with curiosity and resilience, shaping my growth as a researcher. I further want to thank my colleague, Michael Sweeney, with whom I collaborated for two years to build this simulation tool.

Additionally, large parts of this project were funded by the Georgia Tech College of Sciences and the National Science Foundation (NSF) grants #1745584, #1851843, #2244427. Lastly, I want to acknowledge my family and friends that encouraged me through this process: Krishnan Gopalakrishnan, Dr. Suneeta Krishnan, Ketaki Uma Krishnan, and Lauren Sabo. Without their unwavering support, suggestions and phone calls across the Atlantic, this thesis would not have been possible.

Table of Contents

Abstract

Pseudomonas aeruginosa is a notorious opportunistic pathogen that forms aggregates, which play a crucial role in its pathogenesis and antibiotic resistance. Despite their significance, the growth dynamics of these aggregates remain unclear, hindering the development of effective therapeutic strategies. Most existing simulations remain focused on biofilm growth and maintenance, ignoring the dynamics of suspended aggregates. This dissertation presents a multi-scale agent-based simulation approach to model the growth dynamics of P. aeruginosa aggregates. We develop a comprehensive framework that bridges the gap between cell-level interactions and aggregate behavior, balancing biological accuracy with computational efficiency. The simulation aims to capture the interactions between bacterial motility, adhesion, nutrient availability and spatial limitations in shaping aggregate growth. This work has significant implications for the design of novel antibacterial therapies and the development of predictive models for P. aeruginosa infections.

Introduction

Microbial modeling has conventionally focused on the study of planktonic bacterial cells and their interactions and dynamics in mostly homogenous spatial environments (Donlan, 2002). Past research has yielded insights about the nature of intercellular interactions and the dynamics of individual bacterial cells. Over the last few decades, focus has shifted towards the study of biofilms – high-density, surface-attached bacterial colonies enclosed in an extracellular polymeric substance (EPS) matrix. In healthcare, water, and food distribution settings (amongst others), biofilms pose a grave danger to public health and research has targeted the regulation and prevention of their growth (Donlan, 2002). However, considerably less research has been conducted into the dynamics of a different microbial structure that is not attached to any surface, known as bacterial aggregates (Melaugh et al., 2023). An expanding body of research suggests that bacteria – particularly those that are pathogenic to humans – spend significant time in suspended multicellular aggregates. These aggregates exhibit many of the same troublesome characteristics as biofilms, including increased virulence, antibiotic resistance, and tolerance to immune responses.

One of these aggregating bacteria is *Pseudomonas aeruginosa*, a gram-negative, aerobic-facultatively anaerobic bacteria that is pathogenic to humans, particularly immunocompromised individuals (CDC, 2019). Aggregates of *P. aeruginosa* form in several different ways, the primary processes being diffusive aggregation and clonal aggregation (Melaugh et al., 2023). *P. aeruginosa* has been shown to grow slower in biofilms, a trait that has been attributed to decreased rates of nutrient and vitamin diffusion through the EPS matrix, space constraints, and resource competition (Stewart and Franklin). Recent data suggest that this may not be necessarily true for aggregates. This inspires several questions: what are the underlying dynamics that drive larger

aggregates to grow faster than smaller aggregates, and does the tension between separation and growth affect this trend? What social behavior might further influence aggregate growth? To answer these questions efficiently, it is optimal model the formation and interactions of bacterial aggregates in heterogenous spatial conditions, with realistic environmental constraints. While there are many mathematical approaches to modeling spatial structure such as PDEs or graphs, this study will take an agent-based model approach.

The primary objective of this investigation is to develop a computationally efficient simulation platform, capable of modeling suspended aggregates in a biologically relevant manner. An individual-based modelling approach is an ideal candidate for this task due to its ability to capture both individual cell behavior and aggregate-level processes. This thesis explores the ways in which an efficient novel simulation tool can be developed while capturing multi-scale dynamics. It will further demonstrate how the multi-scale nature of individual-based models can be leveraged to optimize the tool. This paper describes the methods of modeling important processes such as diffusive aggregation, clonal aggregation, resource uptake, and public good production (Becker et al., 2018). The goals of this simulation platform are to expand biologists' understanding of the growth dynamics of low-density, antibiotic-resistant bacterium, and present a useful tool to identify factors that may inhibit their growth and pathogenicity.

Literature Review

2.1 *Pseudomonas aeruginosa* as a model organism

Pseudomonas aeruginosa is a major human pathogen targeting those with moderate to severely compromised immune systems. Bloodstream infections (BSI) brought about by the bacterium are associated with high morbidity and possess mortality rates of between 18 – 45% (Reynolds & Kollef, 2021). It has been further demonstrated that antimicrobial resistance increases the mortality rates associated with BSIs contracted due to the bacterium. While biofilms of *P. aeruginosa* have been studied extensively, the bacterium has also been seen to form multicellular aggregates when cultured in liquid media. It is suspected that these aggregates play a key role in disease and eventual biofilm formation (Melaugh et al., 2016). Multi-drug-resistant strains of the bacterium have been identified in a variety of settings, but most prevalently on contaminated equipment and surfaces in medical environments.

The growth of *P. aeruginosa* is mediated by various public goods – in addition to naturally-occurring nutrient in the environment – that are produced in higher concentrations in larger aggregates. It has also been demonstrated that this bacterium uses chemical signaling through the well-studied Type VI secretion system (T6SS), which has been shown to favor the evolution of public goods cooperation (McNally, 2017). Consequently, the proliferation of *P. aeruginosa* from low-density microbial aggregates to antibiotic-resistant biofilms has become a standard case study for those investigating microbial growth dynamics (Thi et al., 2020). The summation of these properties makes P. aeruginosa an excellent candidate for multi-scale simulation modeling of bacterium growth dynamics.

2.2 Modeling cell and aggregate properties

In vitro and *in silico* studies of aggregate formation in *P. aeruginosa* have demonstrated the most important processes that mediate the growth of bacteria from planktonic cells to aggregates. These processes can be broadly classified into two classes. The first class describes physical processes occurring between aggregates such as diffusive aggregation, clonal aggregation, and cell shedding. Melaugh et al. demonstrated that the *de novo* presence of aggregates in exponential-phase cultures are distinguished by a combination of clonal and diffusive growth (Melaugh et al., 2023). Considering the findings of Melaugh et al. and Kragh et al., there is a distinction between the process of aggregation in late-log/stationary-phase cultures and exponential-phase cultures (most likely motivated by high sensitivity to the initial distribution of aggregates present in the culture) (Kragh et al., 2016). However, it is not clear how clonal and diffusive aggregation share the responsibility of mediating aggregate growth and development.

On the other hand, cell death and cell shedding of *P. aeruginosa* aggregates are much better documented processes; Schleheck et al. evidence the notion that aggregates begin to shed cells once they achieve some critical size or in response to environmental stressors (Schleheck et al., 2009). Specifically, Schleheck et al. note that cell dispersal is triggered by the "depletion of limited growth substrate". This class of physical processes provides the basis for a first hypothesis regarding the relationship between aggregate size and aggregate growth rate that this study's simulation will test: the presence of larger, faster-growing aggregates is primarily driven by cells multiplying faster than they separate.

The second class describes the interactions of extracellular substances that exist within the environment such as public goods – products of cell/aggregate processes – and chemicals like antibiotics that are commonly present in an infection space. The

production of public goods like the siderophore Pyoverdine by *Pseudomonas* has been seen to behave as a mediator of aggregate growth. Pyoverdine has been shown to be a determining factor in the bacterium's potential for pathogenesis by facilitating iron extraction which damages host mitochondria, resulting in mitochondrial turnover via autophagy (Becker et al., 2018). Becker et al. provides evidence that the "growth rate [of *Pseudomonas aeruginosa*] increases almost linearly with increasing pyoverdine concentration. The data from Becker et al.'s study suggests that the growth benefit of public goods can be accurately approximated using a modified Hill function.

Regarding the effect of added chemicals on the other hand, there is more experimental evidence as opposed to mathematical models that describe the effect of various antibiotics upon aggregates. Primarily, the broad-spectrum antibiotic ciprofloxacin has been shown to inhibit the growth and structural integrity of *P. aeruginosa* biofilms (Soares et al., 2019). According to Soares et al., exposure of biofilms to ciprofloxacin result in greatly diminished cell viability and disruption of the biofilm's EPS architecture. These findings were similarly reinforced by Yasir et al. who showed that ciproflaxin – in combination with sub-inhibitory concentrations of antimicrobial peptides – was highly effective at thinning pre-formed biofilms (Yasir et al., 2020). In combination, this class of chemical processes provide a secondary hypothesis to that offered by the first class of physical processes: the presence of larger, faster growing aggregates is primarily driven by cooperative behavior that is more effective in larger aggregates and can be inhibited by antimicrobial chemical agents.

2.3 Individual-based models and cell-agent-based model frameworks

Cell-agent-based model frameworks (CABMFs) or individual-based models (IBMs) – the latter being the more commonly used term in microbiology – are a class of

computational models that focus on modeling the interactions and behavior of autonomous individuals within a population (Cornell et al., 2019). The behavior of individual "agents" is described by an underlying set of rules. These rules may vary from discrete conditional statements describing the actions of an agent, to ordinary differential equations (ODEs) modeling the growth or decay of an agent. Agents will also generally possess a series of state variables describing attributes such as position, behavioral, or morphological properties.

The benefit of these models is that they capture individual behavior from the bottom-up, but also population-level patterns that emerge as a product of running simulations over protracted periods of time (Railsback, S. F., & Grimm, V., 2011). One of the primary limitations of these models is the lack of constraint on the number of individual processes or agents being tracked, rapidly leading to models that become too complex for mathematical validation and analysis (Bonabeau, 2002). They hence demand a balance between abstraction and accurate approximation of real-life processes. The advantage of pursuing an agent-based approach to modeling aggregate dynamics over other mathematical methods such as partial differential equation models is the ability to capture individual behavior that continuum models lack.

The most successful CABMFs are products developed to solve specific biological problems such as gene regulatory control or biofilm formation. This notion is exemplified by CompuCell3D which originated from the desire to model simple reaction-diffusion systems and now is used widely in the study of angiogenesis and cancer (Cornell et al., 2019). Similarly, BacSim (Kreft et al., 1998) and its successor iDynoMiCS (Lardon et al., 2011) began primarily from a desire to integrate cell processes into a generic population model and now both serve as a popular tool for the study of biofilm formation and microbial competition. While there are myriad CABMFs,

each providing a useful tool to model bacterial populations, very few simulations focus on the multi-scale modeling of bacterial aggregates, with most existing simulations targeting biofilm formation and dynamics. There is hence widespread demand for a tool that captures both cell-level and aggregate-level behavior in a spatially heterogenous infection environment, particularly as interest in low-density microbiology continues to grow.

Model Description

Historically, agent-based simulations lacked a standardized description that was suitably accessible for audiences lacking a computational background. Introduced by Grimm et al. in 2006, the ODD (Overview, Design Concepts, Details) protocol has become the gold standard for documentation of agent-based frameworks, particularly within ecology. An adapted ODD format is used here to systematically describe the agents, processes, models and submodels of the novel simulation described in this thesis, with the intention of providing both clarity and reproducibility. The simulation was written in Julia with data analysis being performed in Python and MATLAB.

3.1 Purpose

The purpose of this model is to explore non-surface attached aggregate growth dynamics under varying environmental conditions such as resource availability and chemical interactions. It additionally aims to capture the social dynamics of growth through the simulation of public good production. The impetus for developing this simulation stemmed from the desire to understand the relationship between aggregate growth and density, and how environmental and social processes may affect this relationship. However, this simulation is intended to go beyond these questions, ultimately providing biologists with a multi-purpose platform enabling deductions regarding aggregate and cellular growth distributions, and comparisons of population parameters with empirical data.

3.2 Entities, State Variables, and Scale

The primary entities described in this model are bacterial cells, bacterial aggregates, and the 'infection space' of the simulation. Bacterial cells are explicitly defined as the smallest agents within the simulation; their state is defined by continuous *(x, y)* positions within the simulation space, and parameters describing maximal

resource-dependent cell growth, cell death, and the cell dispersal rate (describing the rate at which cells are dispersed from the aggregate they were formerly a part of.)

Aggregates are characterized by size and composition, defined by a set of cell objects and differentiated visually by unique hexadecimal color codes. They possess several state variables including aggregate size (described by the total number of cells within the aggregate), a density-dependent aggregate diffusion rate, as well as a threshold density at which aggregates begin shedding cells and a threshold distance necessary for diffusive aggregation (aggregate collision). While cells have dedicated state variables corresponding to their position in space, aggregate positions are tracked by an 'aggregate density map', which is updated at each simulation time step.

The infection environment is described by layers of 'environmental lattices'; a lattice is a 2-dimensional matrix representing the distribution of the concentration of a chemical (such as a resource, antibiotic, or public good). In conjunction these lattices are leveraged to allow users to emulate a heterogeneous spatial environment. All environmental lattices are distinguished by their ability to modify the rate of growth, death, and aggregation of individual cells. At each time step, continuous cell positions are mapped to discrete spatial segments within the simulation space whose size are defined individually for each environmental lattice. In this manner, the local concentrations of chemicals can be evaluated at each time step for each bacterial agent and the corresponding growth, death or aggregation effect of each chemical can be assessed and updated. The sole constraint on the dimensions of these environmental lattices is that all components must perfectly divide the dimensions of the simulation space.

3.3 Process Overview and Scheduling

Discrete time was selected over discrete event with the intention of improving biological accuracy by capturing simulation processes that may occur simultaneously. A

global time step is initialized at the start of each simulation run. At each time step, cell agents are considered individually, and the following processes are evaluated in order: cell movement, cell death, cell dispersal, and cell division. A static copy of the simulation state is saved at the start of each time step to ensure continuity when calculating the successive state of the simulation. At the conclusion of this loop, diffusive aggregation (aggregate 'collision') as well as the diffusion and decay of each environmental lattice is computed.

1. **Cell Movement** – movement is the sole process defined as an aggregate-level function. An x and y component of direction are selected randomly for each aggregate and the magnitude of diffusion is scaled by the density of the aggregate. This encapsulates a simplistic but effective random walk model of density-dependent aggregate diffusion.

2. **Cell Death** – cells die naturally due to resource availability or at the hands of anti-bacterial agents. Agents are deleted from the simulation via this process and aggregate size parameters are updated as their cells die.

3. **Cell Dispersal** – at each time step, cells possess the ability to leave their current aggregate to seed their own aggregate. The probability that aggregates shed cells increases significantly once aggregates cross a threshold of 'critical density' (a user-defined parameter) beyond which cohesive forces of aggregation are overcome.

4. **Cell Division** – each set of cell processes concludes with cell division. In the case that cell division occurs, either clonal aggregation takes place and the current aggregate's size is incremented, or the new cell is shed and seeds a new aggregate.

Beyond these procedures, the simulation models environmental processes concerning the diffusion, uptake, and decay of chemicals and resource. These are described as submodels below in **Section 3.6.**

3.4 Design Concepts

While the ODD protocol recommends the description of numerous design principles, several concepts on Grimm et al.'s list have no basis in this model. Instead, this section concentrates upon the principles relevant to this simulation: *emergence, adaptation, sensing, stochasticity, collectives, observation.*

3.4.1 Emergence

The most notable emergent property of the model is the formation of aggregates from planktonic cells via either clonal or diffusive aggregation. Aggregation is not directly imposed by the simulation but rather arises naturally from stochastic cell-level processes like movement, resource consumption, cell division, etc. In a similar vein, the public good production-consumption system may be described as an emergent property. While no explicit cell signaling/quorum sensing model was implemented, larger aggregates are modeled to produce public good in greater concentrations and incur a growth cost by doing so. This facilitates emergent social behavior that may lead to unique community dynamics of competition between agents.

3.4.2 Sensing and Adaptation

Cell behavior is adjusted in response to their local chemical environment and to other cells and aggregates in their vicinity. Agents may only sense their immediate surroundings, defined by the specific space they occupy within the spatial lattice of the environment. Agents that find themselves in resource-rich environments grow more rapidly and adjust their growth and death rates according to the concentration of antibiotics or public goods that are present.

3.4.3 Stochasticity

Cell processes like movement, division, death and aggregation are all probabilistic processes. The outcome of each process depends on a combination of local environmental conditions and random chance, leading to variability in the behavior of individual cells and aggregates. We simulate stochasticity via the Gillespie algorithm (citation) to track and evaluate multiple processes at each discrete time step. Each process is modelled in the following manner:

1. Evaluate environmental/cell/aggregate parameters involved in a process and calculate a probability threshold value, p.
2. Sample an independent identically distributed random variable, $0 \leq u \leq 1$.
3. If $u < p$, then the process takes place, otherwise it does not.

Several processes are deterministic – resource decay, chemical diffusion, and so on – however these processes are affected by other stochastic processes such as resource uptake. In this respect, the simulation is predominantly stochastic and each run with the same parameters will produce unique data though the steady-state outcome will be consistent.

3.4.4 Collectives

Aggregates can be considered as collectives of individual cells. The behavior of an aggregate in the model is shaped by the actions of its constituent cells, particularly in terms of public good production, resource consumption and division. At a higher level, the model also captures interactions between different aggregates, particularly through processes of such as aggregate merging and resource consumption.

3.4.5 Observation

A central feature of the simulation is the built-in data collection functionality that saves emergent information from the simulation. Users can save size and growth

rate distributions at an aggregate level, and the spatial distribution of resource over time. While the effective aggregate growth rate, r_i^t , can be described in several different ways, the simulation estimates this metric as the average probability of cell division for a constituent cell of an aggregate (*Equation 1*).

$$r_i^t = \frac{\sum_{j=1}^{c_i^t} r_{i,j}^t}{c_i^t}$$

Equation 1. Effective aggregate growth rate

Effective aggregate growth rate and size distributions are saved as tuple pairs in a plaintext file with minimal formatting. Space delimiters are used to separate time steps and a new plaintext file is created and saved for each run of the simulation.

Furthermore, existing functionality also permits users to save and visualize the distribution of resource at each time step in a similar format. Based on the "SAVE_RESOURCE_GRANULARITY" parameter, a user can define the interval length at which the resource lattice is saved.

Lastly, for any run, users may visualize cell movement via a dynamic density graph which may be toggled on or off. This feature is an excellent addition to the simulation's observation toolkit since it permits the study of behavior in both a qualitative and quantitative manner. Should agents be forming extremely large aggregates or failing to reach resource available at the boundaries of the simulation, this visualization capability enables users to identify this spatial behavior quicker than if they plodded through the aggregate size distribution data.

3.5 Initialization and Inputs

Users are responsible for defining over 40 parameters at the outset of a simulation run (see Appendix for parameter table). These parameters govern the rates of chemical reactions, probability thresholds of cell and aggregate processes, as well as the boundary conditions of the simulation space. Additionally, should users wish to collect statistics

from an experimental run, aggregate and resource data saving can be turned on and target destinations for data files must be specified. The initialization of the resource environment should also be considered by users when preparing the simulation for a run. Resource availability drives the growth of aggregates, and users can opt to either initialize a uniform distribution of resource (where the magnitude of resource concentration can be adjusted), a random distribution of resource, or a user-specified distribution. Lastly, public goods and antibiotics can be optionally toggled on/off as required.

3.6 Submodels

Here, a mathematical overview of the primary simulation sub-processes is presented.

3.6.1 Simulation Environment

The simulation environment $\boldsymbol{\Omega_{envir}}$ is defined as a 2-dimensional lattice, $\boldsymbol{L(x,y)}$, where users can specify the positive and negative limits of both the vertical and horizontal components. Complementary to the simulation lattice, a resource lattice, $\boldsymbol{R(x,y)}$ and additional solute lattices (public goods, added chemicals, etc.) are initialized. Each lattice is divided into a grid where each grid cell is defined via a 'lattice spacing' parameter, which describes the length of the smallest subunit of the simulation space. To identify the number of cells in each direction, we calculate the 'lattice resolution' of the simulation space via Equation 2.

$$\text{lattice\_resolution\_x} = \frac{\text{pos\_lim\_x - neg\_lim\_x}}{\text{lattice\_spacing}}$$

Equation 2. Calculation of lattice dimensions in the x direction

While simulation processes depend upon knowledge of the lattice cell occupied by an agent, agents themselves are off lattice; an agent occupies a position $\boldsymbol{p} = (\boldsymbol{p_x}, \boldsymbol{p_y})$ in continuous $(\boldsymbol{x,y})$ space. This location in continuous space corresponds to a lattice position, $\boldsymbol{\hat{p}}$, which is evaluated each time lattice coordinates are required.

$$\hat{p} \approx \left(\frac{p_x + |\text{neg\_lim\_x}|}{\text{spatial\_step}}, \frac{p_y + |\text{neg\_lim\_y}|}{\text{spatial\_step}} \right)$$

Equation 3. Calculation of lattice coordinates from continuous coordinates.

It is also important to consider the boundary conditions of the simulation space – the freedom of agents to move in or out of the environment in certain directions can greatly affect the outcomes of a simulation run. Currently, there are three boundary types that may be selected: reflective, periodic or Neumann boundary conditions. This enables flexibility with respect to how agents enter/leave a space; either agents will 'reflect' off the walls of the environment, wrap around to the other side of the environment (mimicking infinite space), or leave permanently. Solute and resource lattices are defined to have identical dimensions and boundary conditions as the environmental lattice. The primary considerations for these lattices are consistency regarding their physical properties and ensuring that the spatial step and rates of diffusion are sufficiently small to provide a stable solution to the reaction-diffusion equations that govern solute dynamics (see equation ...).

3.6.2. Solute Dynamics

Solutes in the simulation are modeled by solving the diffusion equation using a forward time-centered space (FTCS) scheme. This method approximates the change in solute concentration across both the x and y directions of the lattice at each time step. Solute diffusion is given by the following equation, where $\boldsymbol{C(x, y, t)}$ is the concentration of solute at position $\boldsymbol{(x, y)}$ and time $\boldsymbol{t}$, $\boldsymbol{D}$ is the diffusion coefficient:

$$\frac{\partial C}{\partial t} = D\left(\frac{\partial^2 C}{\partial x^2} + \frac{\partial^2 C}{\partial y^2}\right)$$

Equation 4. Diffusion Equation.

Equation 4 is simplifed using the concept of *flux* from Fick's First Law (Fick, 1855), whrere solute flux is described in terms of the solute concentration gradient (see Equation 5). $\boldsymbol{\nabla C}$ describes the gradient of the 2-dimensional solute field.

$$J = -D\nabla C$$

Equation 5. Fick's First Law.

Flux is substituted into the general form of the diffusion equation to produce a proportionality relationship which states that the rate of change of solute is proportional to the laplacian of the solute concentration field.

$$\frac{\partial C}{\partial t} = -\nabla \cdot J$$

Equation 6. Substitution of flux into diffusion equation.

The numerical solution of this equation is obtained by discretizing Equation 6 in space and time. Discretizing in the x and y directions and combining the terms produces Equation 7.

$$\Delta C_{x,y} = -\frac{D}{\Delta x^2}(C_{(x+1),y} - 2C_{x,y} + C_{(x-1),y}) - \frac{D}{\Delta y^2}(C_{x,(y+1)} - 2C_{x,y} + C_{x,(y-1)})$$

Equation 7. Discretization.

The stability of the numerical solution is given by Equation 8. When selecting one's time step, diffusion coefficient and lattice spacing parameters, it is critical that consideration is given to their relationship, so that the stability of the solution to the diffusion equation is ensured.

$$\Delta t \leq \frac{\text{lattice\_spacing}^2}{D}$$

Equation 8. Stability condition for numerical solution of diffusion equation.

3.6.3. Population Dynamics

Table 1 gives the primary describes the primary processes that determine population growth, death, and movement in the simulation environment, Ω_{envir}, containing a_t aggregates with c_t^i cells in aggregate $i = 1, \ldots, a_t$ at time step t. The parameters referred to in Table 1 are defined as follows: d is the death rate, β is the post- division separation rate, b is the cell erosion/dispersal rate, ρ is the diffusive aggregation rate within a radius of d_{agg} , and D_a is the density-dependent rate of diffusion of aggregate i. Additionally, k_R is the half-maximal resource concentration and μ_R is the maximal bacterial growth rate.

Biological Process	Mathematical Significance	Process Rate
Cell division/Population growth	$c_i \rightarrow c_i + 1$	$\mu_R \frac{R}{k_R + R} \cdot \Delta t$
Cell separation following division	$a \rightarrow a + 1$	$\beta \cdot \Delta t$
Cell death	$a \rightarrow a + 1, \quad c_i \rightarrow c_i - 1$	$d \cdot \Delta t$
Cell dispersal/erosion	$c_i \rightarrow c_i - 1$	$b \cdot \Delta t$
Diffusive aggregation	$a \rightarrow a - 1$	ρ if $\text{dist}(A_i, A_j) < d_{agg}$, 0 otherwise
Aggregate outflow (boundary-dependent)	$a \rightarrow a - 1$	ρ if $(x, y) \notin \Omega_{\text{envir}}$, 0 otherwise
Aggregate movement	$a(x, y) \rightarrow a(x + \Delta x, y + \Delta y)$	$D_a \cdot \Delta t$

Table 1. Cell processes with corresponding equations and rates.

As mentioned above, bacterial population growth is governed by the local concentrations of resource, added chemicals and other solutes. The simulation's resource-explicit growth model – given by equation 9 – is based on Michaelis-Menten

kinetics (Michaelis & Menten, 1913), using the local resource concentration, **R**, to calculate the division probability, **r**, of an individual cell.

$$r = \mu_R \frac{R}{k_R + R} \cdot \Delta t$$

Equation 9. Resource-explicit growth equation.

Following the steps for performing cell processes that was introduced in **Section 3.4.3**, the simulation samples an independent identically distributed random variable $\mathbf{u_r}$ on the interval **[0,1]**. Cell division occurs if $\mathbf{u_r} < \mathbf{r}$. This equation is a template for integrating more processes into the growth equation, for example, as described in **Section 2.2**, the growth of *P. aeruginosa* is mediated by various public goods that are produced in higher concentrations in larger aggregates. Equation 10 describes the production of a public good at lattice position (x, y) as a function of local cell density. The state variable **P** is used to signify a public good, σ_P denotes maximal public good production and ϕ_P denotes half-maximal public good production.

$$P_{x,y} = \sum_{i=1}^{a^t} \sigma_P \cdot \frac{c_i^t}{\phi_P + c_i^t}$$

Equation 10. Public good production.

The growth benefit of a solute like public good can be integrated into Equation 9. Equation 11 demonstrates how this is achieved in the simulation; two new parameters are introduced here, **α**, a scale factor, and **ξ**, the growth cost of producing public good.

$$r = \left(\mu_R \frac{R}{k_R + R} + \alpha \frac{P}{k_P + P} - \xi\right) \cdot \Delta t$$

Equation 11. Resource-explicit growth equation modified with public good terms.

In this manner, the core population growth model is dynamically modified to account for the effects of local antibiotic or anti-aggregation chemicals.

Results

The tests and results described in this section are not comprehensive; parameter selection, antibiotics and several other simulation features were tested by Michael Sweeney can be found in his undergraduate thesis. Furthermore, a comprehensive list of both computational and biological testing will be available at the time of formal release of this simulation (which will be after the publication of this thesis.)

4.1 Computational Efficiency

Simulation efficiency was of primary concern to the development of this tool. Each feature was tested to ensure that its implementation had minimal impact on simulation runtime and computer memory usage. The first iteration of the simulation saved aggregate size and growth rate distributions in an SQL relational database format.

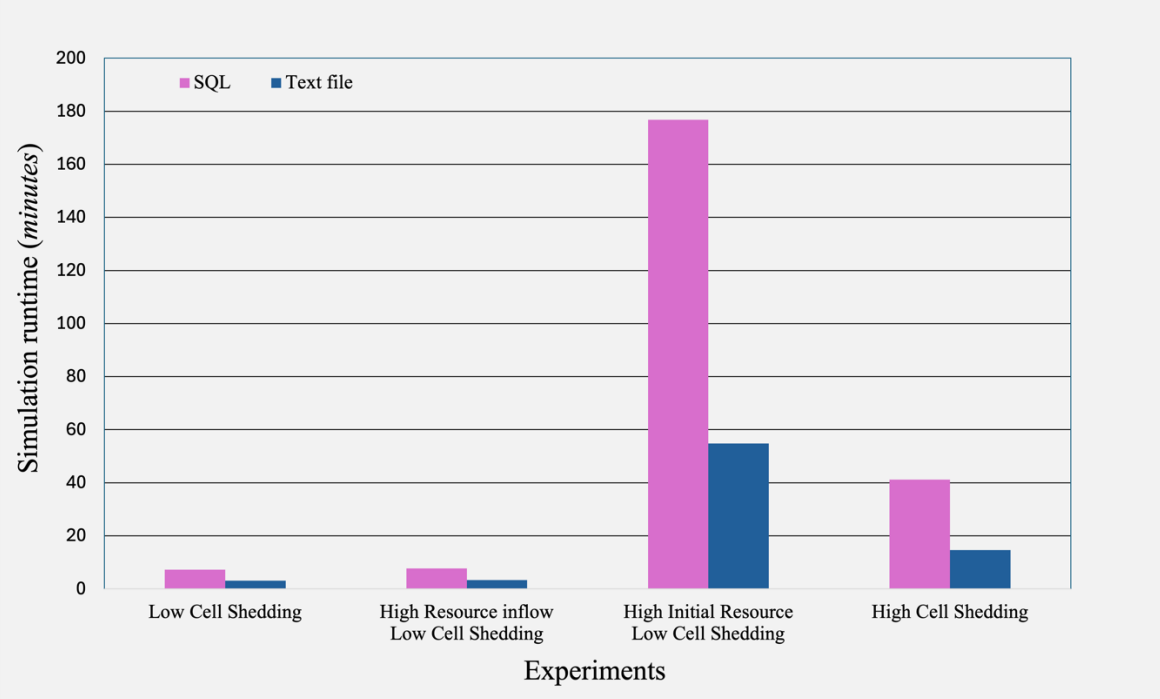

Figure 1. ***Comparing simulation efficiency when saving to SQL versus to text file****. Four experiments were selected with different resource and cell shedding probability values, and average runtime over 100 runs were plotted.*

Though MySQL provided a user-friendly interface and simple select, insert and update commands, it increased the simulation's overhead considerably. As demonstrated in Figure 1, switching to saving data in raw text files reduced simulation runtime significantly, with plaintext being almost 300% faster in the memory-intensive experimental case (high initial resource), while keeping the data in a readable format that is convenient for data analysis.

Saving resource data was the other memory-intensive saving feature that was tested. As indicated by Figure 2, with a save granularity of 50 (i.e. saving the resource lattice every 50 timesteps), even as the number of runs increases, the resource saving feature did not have a notable impact on runtime.

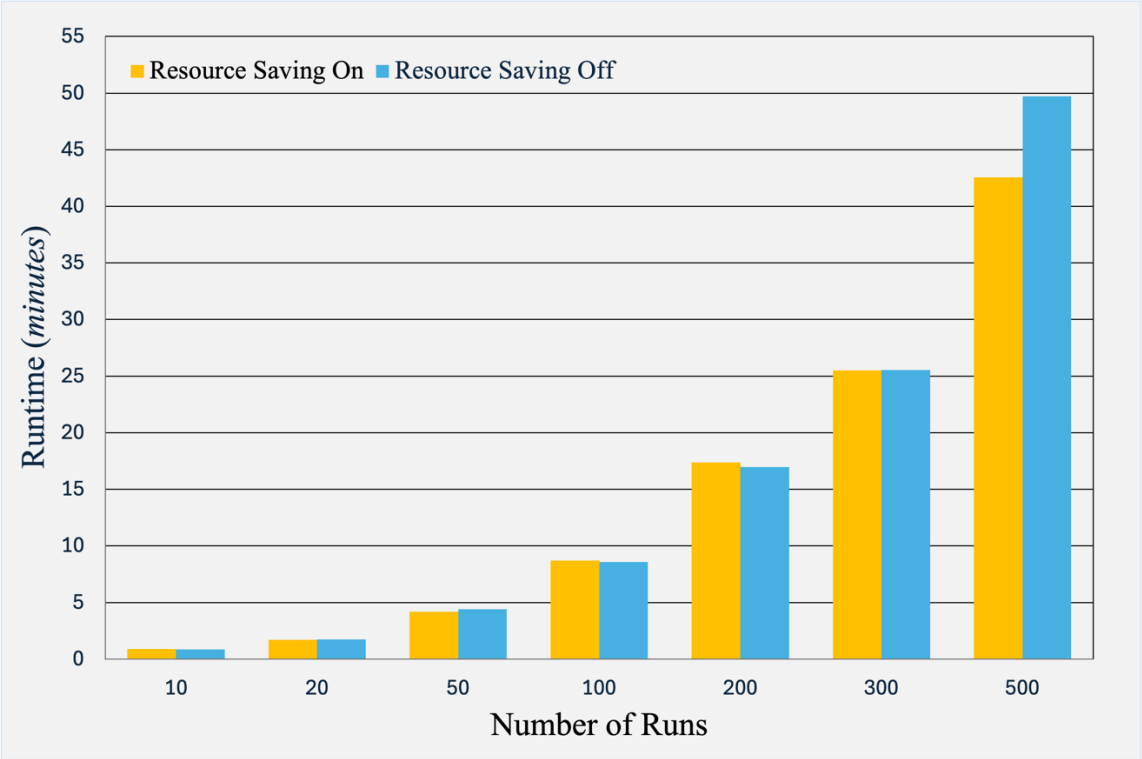

Figure 2. ***Comparing simulation efficiency when resource saving is on against when it is off.*** *Each experiment was run with the same timestep ($\nabla t = 0.01$) and total time (20 hours), with resource being saved every 50 timesteps.*

4.2 Diffusion Mechanics

Solute dynamics were visualized in order to confirm the correctness of the simulation behavior. Resource was initialized in two different scenarios, one with a random initial condition (Panel A in Figure 3) and a second with a point source (Panel B in Figure 3).

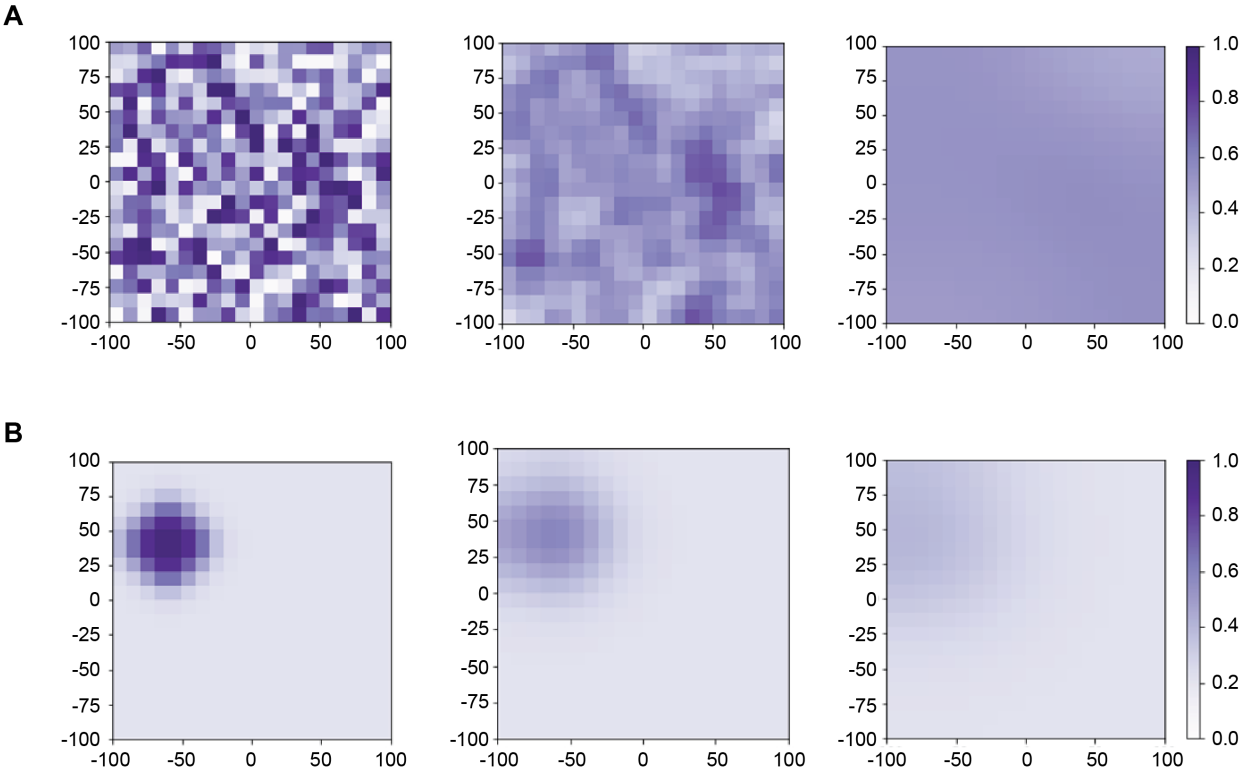

Figure 3. ***Visualizing solute dyanmics****. Panel A displays resource diffusion from a random initial condition. Panel B displays resource diffusion from a point source. Time progresses from left to right.*

Over time, resource diffuses evenly until a steady state equlibrium concentration is reached.

4.3 Biological Validation

Though this thesis is computationally focused, its underlying motivation and goal is to answer biological questions regarding the dynamics of suspended aggregates. While a full

suite of biological testing is beyond the scope of this paper, the primary mechanisms of clonal and diffusive aggregation were tested to validate the model.

4.3.1 Isolating Clonal Aggregation

Diffusive aggregation was turned off to isolate the mechanism of clonal aggregation. Figure 4 demonstrates the low separation case, where the probability of a new cell leaving its aggregate to form its own aggregate was fixed to be low.

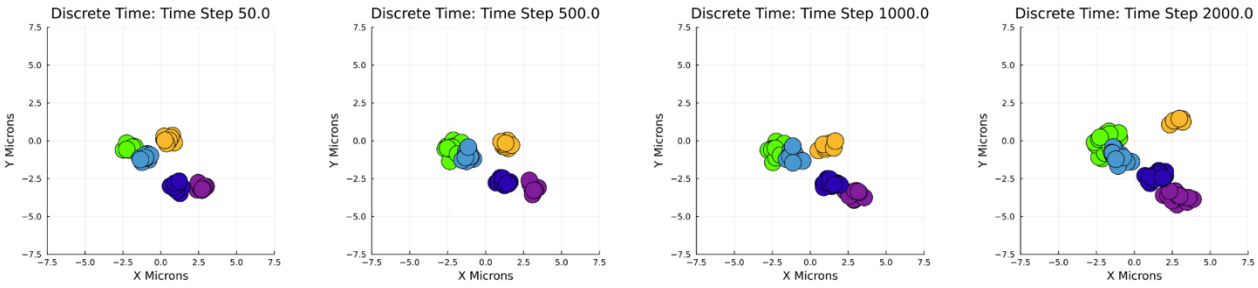

Figure 4. ***Low Separation, no collisions****. An inoculum of 5 aggregates, each with 5 cells, are simulated with a lower fixed probability of a new cell leaving its current aggregate to form a new aggregate. Each color represents a unique aggregate.*

Figure 5 on the other hand fixed the probability of a new cell to form its own aggregate as high. The difference is dramatic. While the number of aggregates remains the same over 2000 timesteps in the low separation case, a high number of smaller aggregates and planktonic cells are visible in the high separation case.

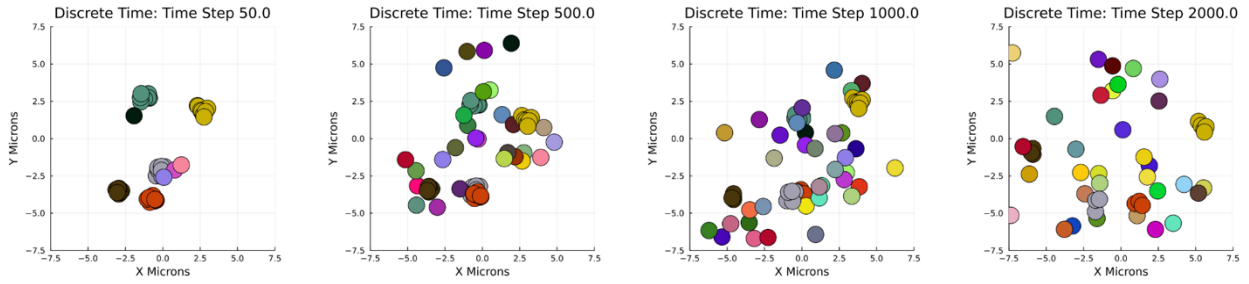

Figure 5. ***High Separation, no collisions****. An inoculum of 5 aggregates, each with 5 cells, are simulated with a higher fixed probability of a new cell leaving its current aggregate to form a new aggregate. Each color represents a unique aggregate.*

4.3.2 Clonal Aggregation with Collisions On

Turning on collisions enabled aggregates to diffusively aggregate into each other, adding another dimension to aggregate interactions. In this case, we see the number of aggregates in Figure 6, the low separation case, to decrease as smaller aggregates merge while clonal offspring remain with their aggregates.

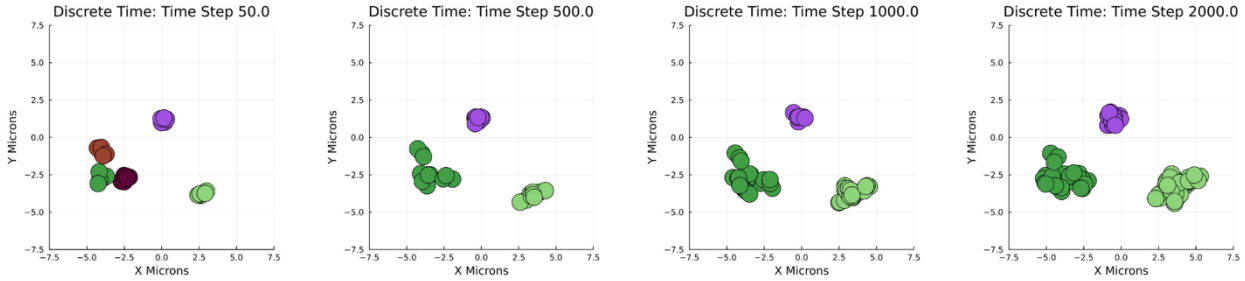

Figure 6. ***Low Separation, with collisions****. An inoculum of 5 aggregates, each with 5 cells, are simulated with a higher fixed probability of a new cell leaving its current aggregate to form a new aggregate. Each color represents a unique aggregate.*

On the other hand, Figure 7 shows how diffusive and clonal aggregate behaviors interact under high separation conditions. While a larger number of aggregates than inoculum indicate that the high separation is continuing to function as expected, collisions being turned on enables cells that have separated from their parent aggregate to re-aggregate at times.

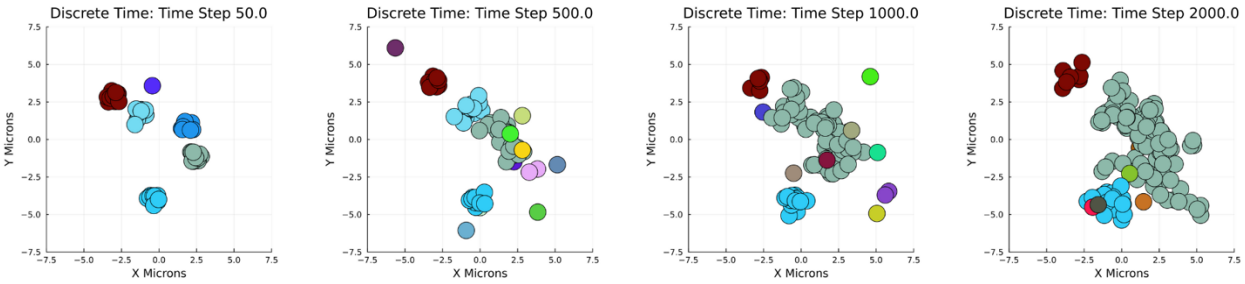

Figure 7. ***High Separation, with collisions****. An inoculum of 5 aggregates, each with 5 cells, are simulated with a higher fixed probability of a new cell leaving its current aggregate to form a new aggregate. Each color represents a unique aggregate.*

Typically, cells of *P. aeruginosa* have directed movement with cells that disperse from their parent aggregates being able to move away and in different directions. Since the

simulation lacks this directed movement currently, these figures represent predictable emergent behavior.

Discussion

5.1 Key Findings

This study demonstrated that the model performs well both in terms of computational efficiency and biological relevance. The transition from SQL to plaintext data saving, significantly reduced overhead and made it feasible to run longer-scale simulations without performance bottlenecks. At the same time, the core biological mechanisms—clonal aggregation and diffusive aggregation—were successfully modeled and visualized, producing behavior that reflects known microbial dynamics in suspended biofilm environments. The combination of computational speed and emergent biological behavior highlights the utility of the simulation as a flexible, performance-focused research tool. While the simulation is still resource-intensive when run on a single processor, using multi-threading or a server with several cores would likely raise the computational ceiling for the model.

From a biological perspective, the simulation was able to isolate and demonstrate the effects of key mechanisms governing aggregate behavior. In the clonal aggregation tests with no collisions, low separation probabilities produced stable, well-defined aggregates that persisted across time. Conversely, under high separation rates, the simulation produced dispersed and numerous smaller aggregates, reflecting early stages of biofilm dispersal or planktonic behavior. When collisions were enabled, more dynamics emerged: in the low separation case, aggregates merged over time due to proximity-driven interactions, while in the high separation case, the overall number of aggregates still increased, but occasional merging events were observed. This reaggregation behavior emerged despite the absence of directional movement, suggesting that the basic rules implemented can still yield biologically plausible outcomes.

5.2 Limitations

That said, there are many limitations to the current model. These include the lack of directed movement and the abstraction of many metabolic cell processes. Additionally, while this thesis validated the clonal and diffusive behaviors of the model, many other components—such as antibiotic interactions, quorum sensing, and environment-specific constraints—remain to be tested or fully integrated. Given that they are beyond the scope of this thesis, this testing will be further documented at the time of this simulation's formal publication. Further biological validation, ideally through comparison to experimental data or known microbial behavior under lab conditions, is necessary to support the broader use of this simulation as a predictive or hypothesis-generating tool.

Conclusion

This thesis presents the development, initial validation and testing of a computational modeling tool aimed at studying the dynamics of suspended aggregates of *Pseudomonas aeruginosa,* balancing biological fidelity and computational efficiency. This study implemented a successful discretization of the diffusion equation and integration into a resource-explicit growth scheme. Both intentional and emergent aggregate behavior was observed during model testing. Future work should address these limitations by introducing space and volume constraints, adding directed movement, and testing the suite of biological features present in the model. On the computational side, further optimization like multi-threading could improve the speed and usability of this tool.

Overall, this simulation offers a promising platform for in silico experimentation, capable of producing accurate and emergent microbial behavior with reasonable computational demands. This study exemplifies the utility of agent-based modeling for capturing biologically accurate behavior at different resolutions while remaining efficient. It serves as a foundation for future investigations and will be further validated and expanded after this thesis to support further research into the dynamics of suspended aggregates.

References

Becker, F., Wienand, K., Lechner, M. *et al.* Interactions mediated by a public good transiently increase cooperativity in growing *Pseudomonas putida* metapopulations. *Sci Rep* **8**, 4093 (2018). https://doi.org/10.1038/s41598-018-22306-9

Bonabeau, Eric. "Agent-based modeling: Methods and techniques for simulating human systems." Proceedings of the National Academy of Sciences, vol. 99, no. suppl_3, 14 May 2002, pp. 7280–7287, https://doi.org/10.1073/pnas.082080899.

Centers for Disease Control and Prevention. (2019, November 13). *Pseudomonas aeruginosa infection*. Centers for Disease Control and Prevention. https://www.cdc.gov/hai/organisms/pseudomonas.html

Cornell, S.J., Suprunenko, Y.F., Finkelshtein, D. *et al.* A unified framework for analysis of individual-based models in ecology and beyond. *Nat Commun* **10**, 4716 (2019). https://doi.org/10.1038/s41467-019-12172-y

Donlan RM. Biofilms: microbial life on surfaces. Emerg Infect Dis. 2002 Sep;8(9):881-90. doi: 10.3201/eid0809.020063. PMID: 12194761; PMCID: PMC2732559.

Jonathan Naylor, Harold Fellermann, Yuchun Ding, Waleed K. Mohammed, Nicholas S. Jakubovics, Joy Mukherjee, Catherine A. Biggs, Phillip C. Wright, and Natalio Krasnogor Simbiotics: A Multiscale Integrative Platform for 3D Modeling of Bacterial Populations. *ACS Synthetic Biology* **2017** *6* (7), 1194-1210 DOI: 10.1021/acssynbio.6b00315

Kang, J. S., Moon, C., Mun, S. J., Lee, J. E., Lee, S. O., Lee, S., & Lee, S. H. (2021). Antimicrobial Susceptibility Trends and Risk Factors for Antimicrobial Resistance in *Pseudomonas aeruginosa* Bacteremia: 12-Year Experience in a Tertiary Hospital in Korea. *Journal of Korean medical science*, *36*(43), e273. https://doi.org/10.3346/jkms.2021.36.e273

Kragh KN, Hutchison JB, Melaugh G, Rodesney C, Roberts AEL, Irie Y, Jensen PØ, Diggle SP, Allen RJ, Gordon V, Bjarnsholt T2016.Role of Multicellular Aggregates in Biofilm Formation. mBio7:10.1128/mbio.00237-16.https://doi.org/10.1128/mbio.00237-16

Kreft, J.-U., Booth, G., & Wimpenny, J. W. (1998). BacSim, a simulator for individual-based modelling of bacterial colony growth. *Microbiology*, *144*(12), 3275–3287. https://doi.org/10.1099/00221287-144-12-3275

Lardon, L. A., Merkey, B. V., Martins, S., Dötsch, A., Picioreanu, C., Kreft, J., & Smets, B. F. (2011). Idynomics: Next-generation individual-based modelling of biofilms. *Environmental Microbiology*, *13*(9), 2416–2434. https://doi.org/10.1111/j.1462-2920.2011.02414.x

McNally, L., Bernardy, E., Thomas, J., Kalziqi, A., Pentz, J., Brown, S. P., Hammer, B. K., Yunker, P. J., & Ratcliff, W. C. (2017). Killing by type VI secretion drives genetic phase separation and correlates with increased cooperation. *Nature Communications*, *8*(1). https://doi.org/10.1038/ncomms14371

Melaugh G, Martinez VA, Baker P, Hill PJ, Howell PL, Wozniak DJ, Allen RJ. Distinct types of multicellular aggregates in Pseudomonas aeruginosa liquid cultures. NPJ Biofilms Microbiomes. 2023 Jul 28;9(1):52. doi: 10.1038/s41522-023-00412-5. PMID: 37507436; PMCID: PMC10382557.

Railsback, S. F., & Grimm, V. (2011). Agent-Based and Individual-Based Modeling: A Practical Introduction. Princeton University Press. http://www.jstor.org/stable/j.ctt7sns7

Soares A, Roussel V, Pestel-Caron M, Barreau M, Caron F, Bouffartigues E, Chevalier S and Etienne M (2019) Understanding Ciprofloxacin Failure in Pseudomonas aeruginosa Biofilm: Persister Cells Survive Matrix Disruption. Front. Microbiol. 10:2603. doi: 10.3389/fmicb.2019.02603

Thi, M. T. T., Wibowo, D., & Rehm, B. H. A. (2020). *Pseudomonas aeruginosa* Biofilms. *International journal of molecular sciences*, *21*(22), 8671. https://doi.org/10.3390/ijms21228671

Vater, S. M., Weiße, S., Maleschlijski, S., Lotz, C., Koschitzki, F., Schwartz, T., Obst, U., & Rosenhahn, A. (2014). Swimming behavior of Pseudomonas aeruginosa studied by holographic 3D tracking. *PloS one*, *9*(1), e87765. https://doi.org/10.1371/journal.pone.0087765